

Analysis and design of rectangular microstrip antenna on two-layer substrate materials at terahertz frequency

Kumud Ranjan Jha · G. Singh

Published online: 2 June 2010
© Springer Science+Business Media LLC 2010

Abstract In this paper, an effective permittivity of the two-layer dielectric substrate material has been analyzed to enhance the electrical performance of the rectangular microstrip patch antenna at terahertz frequency. The frequency dependent effective dielectric permittivity of the substrate materials has been evaluated and result has been compared with finite integral technique based CST Microwave Studio a commercially available simulator. The input impedance characteristic with electrical performance of the rectangular microstrip patch antenna on two-layer substrate materials has also been analyzed at 600 GHz. Manipulation in the input impedance characteristic of the antenna has led to a slow wave structure. This slow wave structure has been examined at 542 GHz, and improvement in the performance has been observed without increasing the overall dimension of the proposed antenna.

Keywords Microstrip antenna · Dispersive behavior · Terahertz frequency · Two-layer substrate · Slow-wave antenna

1 Introduction

Recent technological breakthrough of the electromagnetic energy radiation sources, components, and devices in the

terahertz regime, which is one of the least explored and most promising region of the electromagnetic spectrum for a growing range of applications [1, 2] such as sensing, imaging and wireless communications, detecting explosive [2] or bio-weapons [3–7] and spectroscopic imaging for biomedical applications could become significant. The potential challenges to terahertz technology include making compact and robust sources and detectors, enabling turnkey application in laboratories of the non-specialist and enhancing the management of terahertz lights through the antennas for both far-field and near-field. Far-field enhancement can be performed by using special broadband antennas. As we know that the antenna is a key component for the wireless communication systems. At terahertz frequency, the implementation of this device is still the matter of exploration. In designing a microstrip antenna at high-frequency, the photonic crystal is widely used as a substrate material [8–11]. Fernandes and Rocha [12] have designed an antenna at high frequency using photonic band gap structure as substrate. However, the design of such antenna at high frequency where component size is reduced is a challenging task. Brown and Parker [13] have proposed to enhance the performance of planar antenna by using photonic substrate, which suffers from high radiation loss. Several researchers [8–13], have investigated the millimeter wave antenna by using the photonic crystals as substrate but the gain of antennas is still low due to the enhancement in the bandwidth of the antenna. However, at such a high-frequency (terahertz) even 10% bandwidth is quite capable of conveying a large volume of the information. Dahele et al. [14] have studied the gain enhancement technique in the lower microwave frequency regime. Halim et al. [15] used electronic bandgap (EBG) structure to enhance the gain of microstrip antenna up to 9 dB at 2.7 GHz. Noghianian and Safai [16] have studied the gain enhancement technique for the annular slot antenna

K.R. Jha
School of Electronics and Communication Engineering,
Shri Mata Vaishno Devi University, Katra,
Jammu and Kashmir 182320, India

G. Singh (✉)
Department of Electronics and Communication Engineering,
Jaypee University of Information Technology, Solan 173 215,
India
e-mail: drghanshyam.singh@yahoo.com

and achieved the directivity up to 11.36 dBi. Nishiyama et al. [17] have studied the effect of stacked microstrip structure for proximity coupled microstrip antenna at 7.5 GHz and have achieved maximum directivity of 9 dBi. Kumar and Singh [18] have studied the input impedance characteristics of the circular patch antenna. To enhance the performance, various multilayer layer substrate antennas have been studied in detail by [19–22], but they all are on the microwave/millimeter region of the electromagnetic spectrum only.

The rectangular microstrip patch antenna at terahertz frequency regime designed on stacked substrate and photonic crystal has been reported in [23–25], which suffers from poor radiation efficiency and gain. Recently, Jha and Singh [26] have reported a rectangular microstrip patch antenna on two-layer substrate materials for surveillance systems in which various types of losses at terahertz frequency is investigated. In [26], the effective dielectric permittivity and losses of two-layer substrate material of a rectangular microstrip patch antenna for communication systems have been analyzed and simulated at terahertz frequency regime. In the present paper, an effective dielectric permittivity of multilayer microstrip terahertz antenna is analyzed and extended to design enhanced gain antennas at 0.5–0.7 THz frequency range of the spectrum. The remainder organization of the paper is as follow. Section 2 concerns with the proposed antenna configuration and analysis of the effective permittivity of the two-layer substrate material. Section 3 discusses about the analytical and simulated results of the proposed antenna. In Sect. 4, the behavior of a slow-wave antenna has been proposed and discussed. Finally, Sect. 5 concludes the work.

2 Analysis

2.1 Antenna configuration

The geometrical configuration of a rectangular microstrip patch antenna is shown in Fig. 1. The antenna is designed on two-layer substrate material of the surface area $400 \times 410 \mu\text{m}^2$. The thickness of lower substrate (PTFE, $\varepsilon = 2.08 \tan \delta = 0.0004$) and upper substrate layer (Arlon AR 600, $\varepsilon = 6.0 \tan \delta = 0.0035$) are $h_2 = 300 \mu\text{m}$ and $h_1 = 100 \mu\text{m}$, respectively. The radiating patch and the ground plane are made of $50 \mu\text{m}$ thick copper. The surface area of radiating patch is equal to $200 \times 200 \mu\text{m}^2$. There are several methods to excite the antenna at the microwave frequency. However, realization of all these techniques at the terahertz frequency is a challenging task due to the reduction in the dimension of the device. Considering this difficulty and to reduce the fabrication error, the microstrip feed-line has been used in the present design. Due to the on planar

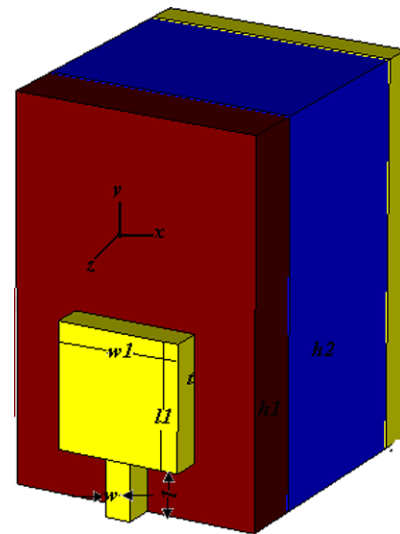


Fig. 1 Geometrical configuration of the proposed rectangular microstrip antenna on two-layer substrate material at terahertz frequency

feeding, the fabrication process of the antenna is simplified. A copper microstrip line of width $40 \mu\text{m}$, length $90 \mu\text{m}$ and thickness $50 \mu\text{m}$ excites this proposed antenna.

2.2 Effective permittivity

As we know that the proper selection of substrate material is the key factor of an antenna design at any frequency range. The output electrical parameters like gain, directivity and radiation efficiency of an antenna is influenced by the selection of substrate material. At microwave frequency, the high dielectric permittivity substrate material is used for the component design. In general, the dimension of a microwave device is a sub-multiple of the guided wavelength. On this way, at the terahertz frequency, size of the device is reduced to the extent where ordinary fabrication process can not meet the dimensional accuracy. With increase in the dielectric permittivity of the substrate, this situation is deteriorated further. To overcome this problem, low-dielectric permittivity material is a potential option. However, practically it has been seen that application of this kind of material leads to the reduction in the gain and enhancement in the cross-polarization of a microstrip antenna. To overcome these problems, two-layer substrate material concept is an excellent choice. In this configuration, upper and lower substrates are chosen as high and low dielectric permittivity material, respectively and the thickness of these materials is selected on such a way that the fabrication error is minimized. Apart from this constraint, another challenge is the high attenuation rate of the signal at the terahertz frequency. In addition to the atmospheric loss, the signal is also attenuated by the component itself in the form of conductor and dielectric losses. To analyze the conductor and dielectric losses at

any frequency, the effective dielectric permittivity of the material is required to be evaluated. At the higher frequency, the effective dielectric permittivity of the substrate is frequency dependent. Recently, we have explored these losses and designed a dual-band microstrip antenna at terahertz frequency in which the effective dielectric permittivity of the material was extracted by using two-capacitance model [26]. In the present work, we have explored the feasibility of improvement in the accuracy of an effective dielectric permittivity of the two-layer substrate material and after successful calculation of the effective dielectric permittivity of the material. We have also studied various electrical performances of the terahertz antenna using this composite dielectric material as the substrate material.

It is well known fact that with the increase in frequency, the behavior of material changes and an effective dielectric permittivity of composite material also changes. In the past, various researchers [27–31] have investigated the dispersive behavior of multilayer substrate but they have been confined to the microwave regime only. Hammerstad and Jensen [32] have devised a formula to calculate an effective dielectric permittivity of substrate material with the high accuracy at low frequency. However, this formula does not take in to account the dispersive behavior of material. Kobayshi [33] has proposed the formula to calculate the frequency dependent effective dielectric permittivity of the composite material. Nevertheless, this formula has also been validated at low frequency (below 100 GHz) and the analysis is based on the single substrate layer. For multilayer dielectric material, two-capacitance model using conformal mapping is frequently used [34]. However, all these formulas are independent and have been investigated in different low frequency regime. In order to calculate the effective dielectric permittivity at the high frequency, we propose to integrate these formulas to obtain new tool to calculate an effective permittivity at terahertz frequency. This value has been calculated by using the two-capacitance model [26]. Since the capacitance is directly proportional to the dielectric permittivity and inversely proportional to the distance between two plates, the relative dielectric permittivity of the composite material is:

$$\varepsilon_{rc} = \frac{d_1 + d_2}{\frac{d_1}{\varepsilon_1} + \frac{d_2}{\varepsilon_2}} \quad (1)$$

where ε_{rc} is the dielectric permittivity of composite material. ε_1 and ε_2 are dielectric permittivity of top and bottom layer of composite material. By using conformal mapping technique d_1 and d_2 are calculated as:

$$d_1 = \frac{K(k_1)}{K'(k_1)} \quad \text{where } k_1 = \frac{1}{\cosh(\frac{\pi w}{4h_1})} \quad (2)$$

$$d_2 = \frac{K(k)}{K'(k)} - \frac{K(k_1)}{K'(k_1)} \quad \text{where } k = \frac{1}{\cosh(\frac{\pi w}{4(h_1+h_2)})} \quad (3)$$

In the generalized way, (2) and (3) have been calculated using approximate formulas [25].

$$\begin{aligned} \frac{K}{K'} &= \frac{1}{\pi} \ln \left(2 \frac{1 + \sqrt{k}}{1 - \sqrt{k}} \right) & 0.7 \leq k \leq 1 \\ &= \left[\frac{1}{\pi} \ln \left(2 \frac{1 + \sqrt{k'}}{1 - \sqrt{k'}} \right) \right]^{-1} & 0 \leq k \leq 0.7 \end{aligned} \quad (4)$$

where $K(k)$ is the complete elliptic integral of the first kind and complementary module $k' = \sqrt{1 - k^2}$. After calculating the value of composite dielectric permittivity ε_{rc} , which behaves as the dielectric constant of equivalent single layer dielectric material, frequency dependent effective dielectric permittivity of composite material is calculated by using the following formula [33].

$$\varepsilon_e(f) = \varepsilon_{rc} - \frac{\varepsilon_{rc} - \varepsilon_e(0)}{1 + (f/f_a)^m} \quad (5)$$

where

$$f_a = \frac{f_b}{0.75 + (0.75 - 0.332\varepsilon_{rc}^{-1.73})w/h}$$

$$f_b = \frac{47.746}{h\sqrt{\varepsilon_{rc} - \varepsilon_e(0)}} \tan^{-1} \varepsilon_{rc} \sqrt{\frac{\varepsilon_e(0) - 1}{\varepsilon_{rc} - \varepsilon_e(0)}}$$

$$m = m_0 m_c \leq 2.32$$

$$m_0 = 1 + \frac{1}{1 + \sqrt{\frac{w}{h}}} + 0.32(1 + \sqrt{w/h})^{-3}$$

$$m_c = \begin{cases} 1 + \frac{1.4}{1+w/h} (0.15 - 0.235e^{-0.45f/f_a}) & \text{for } w/h \leq 0.7 \\ 1 & \text{for } w/h > 0.7 \end{cases}$$

There are various methods to calculate the static effective dielectric permittivity $\varepsilon_e(0)$ of the material at low frequency with certain accuracy. In order to improve the accuracy, we have used S-H formula [32] to calculate $\varepsilon_e(0)$.

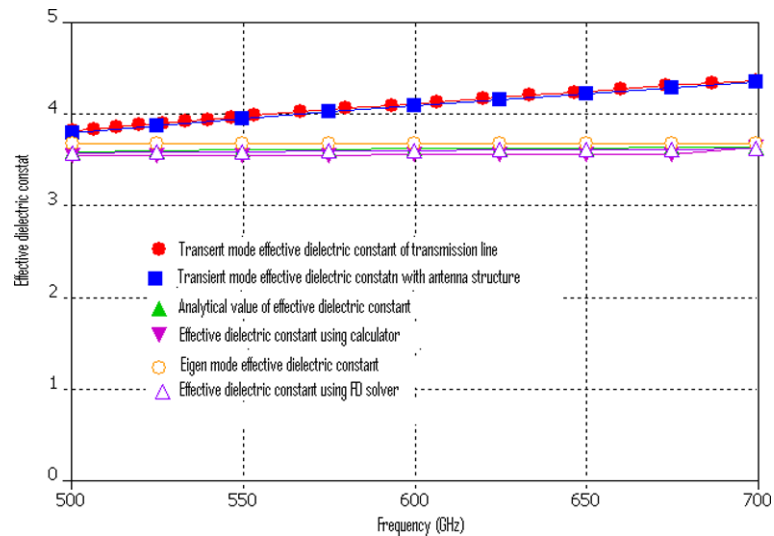
$$\begin{aligned} \varepsilon_e(0) &= \frac{\varepsilon_{rc} + 1}{2} + \frac{\varepsilon_{rc} - 1}{2} \left(1 + \frac{12h}{w} \right)^{-1/2} \\ &\quad + F(\varepsilon_{rc}, h) - 0.217(\varepsilon_{rc} - 1) \frac{t}{\sqrt{wh}} \end{aligned} \quad (6)$$

where

$$F(\varepsilon_{rc}, h) = \begin{cases} 0.02(\varepsilon_{rc} - 1)(1 - w/h)^2 & \text{for } w/h < 1 \\ 0 & \text{for } w/h \geq 1 \end{cases}$$

In the above equations, $h = h_1 + h_2$, w = width of strip-line and t is the thickness of metallization. The frequency f is in GHz. To calculate the effective dielectric permittivity of the composite materials used as substrate in the proposed microstrip antenna as shown in Fig. 1, we have simplified the

Fig. 2 An effective dielectric permittivity of the two-layer substrate materials at terahertz frequency



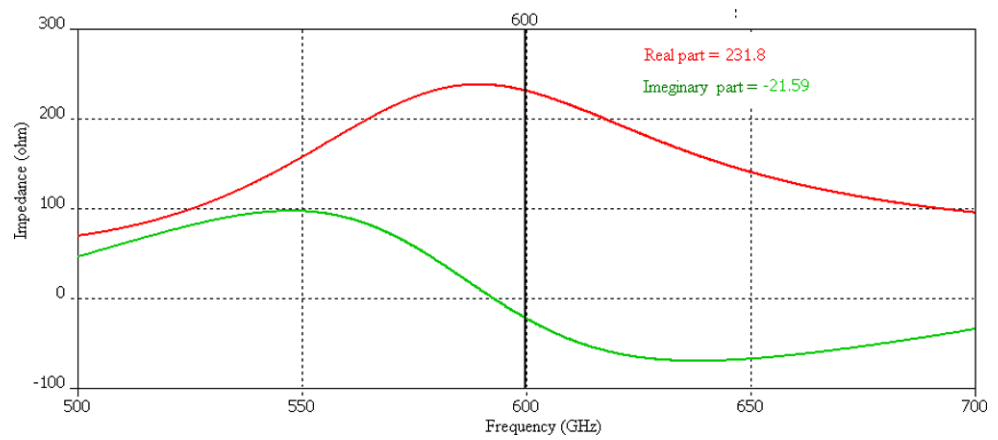
approach and considered only narrow microstrip feed-line placed on the substrate. At the high frequency, in the narrow microstrip line, the current distribution is not uniform and variation in the characteristic impedance is faster in comparison to the wide microstrip transmission line. It indicates that analysis of narrow microstrip line would also predict the behavior of the whole antenna. A microstrip transmission line of 90 μm length and 40 μm width is investigated using (1)–(6) and effective dielectric permittivity of the material is obtained analytically. To validate the analytical result, the effective dielectric permittivity has further been calculated using PACAAD 21 calculator (Sintel Legacy Co.) and finally simulated using different solvers in CST Microwave Studio. The comparison of analytical and simulated results is shown in Fig. 2. In order to simulate the structure using transient solver (space discretized set of Maxwell’s grid equations) in CST Microwave Studio, the microstrip-feed line of the antenna is placed under the open boundary condition except $E_t = 0$ at Z_{min} . In other word, the microstrip feed-line is simulated in the real working condition in place of enclosed boundary condition. Next to this, the structure has been simulated at different discrete frequency points using frequency domain solver (based on Maxwell’s equations in the harmonic case) under the same boundary condition by replacing the two layer dielectric permittivity by single layer of equivalent dielectric permittivity equal to 3.689 obtained using (1)–(4) with total thickness of the substrate equal to 400 μm . Further, the same microstrip line has been simulated using eigenmode solver (based on the eigenvalue equation for non-driven and loss-free harmonic problems). Finally, to investigate the deviation of an effective dielectric permittivity of the material for the proposed antenna, whole structure as shown in Fig. 1, has been simulated using transient mode solver. The comparison of the effective dielectric permittivity of the composite substrate materials obtained by using different techniques is shown in Fig. 2.

Figure 2 reveals that the analytical result is in close agreement with simulated results except in the transient solver. In the transient solver, the substrate materials are stacked as to work in the real environment. In other simulation techniques, a single equivalent substrate material whose permittivity has been obtained by using simple two-capacitance model replaced these two substrates. Generally, in the analysis of the effective permittivity of multilayer substrate, various substrates are represented by its equivalent capacitances. However, these representations need that the material must be sandwiched between two conducting layers but in real practice, these are placed one above the other without any interfacing conducting material. Due to this tolerance, the result obtained by using transient solver, deviates with respect to the analytical result. When an equivalent single layer substrate replaces the two-layer substrate, results obtained by various techniques converge to the analytical result. At the last, when the complete antenna structure is simulated; the effective permittivity is identical to the effective permittivity of the material obtained by considering the narrow microstrip line only. On this way, the frequency dependent dielectric permittivity of multilayer material can be extracted in the terahertz frequency regime to improve the accuracy of the performance.

3 Antenna design

The input impedance of radiating patch is an important parameter to be consideration in designing any microstrip patch antenna. The input impedance of the patch predicts the electrical performance of the antenna. The input impedance of resonating patch is calculated using approximate two-slot conductance method to validate the correctness of an effective dielectric permittivity and to further investigate the

Fig. 3 Variation of the input impedance with frequency (GHz) of the rectangular microstrip antenna



behavior of electrical performance. The radiating edge-slot conductance is approximated as [35].

$$G_1 = \frac{1}{90} \left(\frac{w_1}{\lambda_0} \right)^2 \quad (7)$$

$$G_{12} = \frac{1}{120\pi^2} \times \int_0^\pi \left[\frac{\sin\left(\frac{k_0 w_1}{2} \cos \theta\right)}{\cos \theta} \right]^2 J_0(k_0 L_1 \sin \theta) \sin^3 \theta d\theta \quad (8)$$

and

$$R_{in} = \frac{1}{2(G_1 \pm G_{12})} \quad (9)$$

where w_1 , λ_0 , k_0 , L_1 and J_0 are width of radiating patch, free space wavelength, free space wave-number, length of radiating patch and first kind of zero order ordinary Bessel function, respectively. However, the value of G_{12} can be neglected if the distance between two slots is large as the effect of mutual coupling is negligible. In the present proposed design, the length of patch is greater than $\lambda_g/2$ at 600 GHz and on this way, the mutual conductance is negligible. The calculated value of input resistance under the resonance condition at this frequency is equal to $R_{in} = 282 \Omega$ and associated reactance must vanish at the resonance frequency. To analyze this effect, the radiating patch is excited at the one of the radiating edge and simulated value of impedance is shown in Fig. 3. It is revealed from Fig. 3 that the actual resonance occurs at about 598 GHz where the reactive component is equal to zero. At the intended frequency 600 GHz, the value of impedance is equal to $231.8 - j21.59 \Omega$. The real part of the impedance moderately varies from the analytical result. In the narrow microstrip patch at the high frequency, the distribution of the current density is non-uniform and due to this, the impedance value changes sharply. However, these two results give a good approximation of the input impedance seen by the microstrip feed-line if placed at the edge of the patch. The capacitive reactance as shown in Fig. 3 is

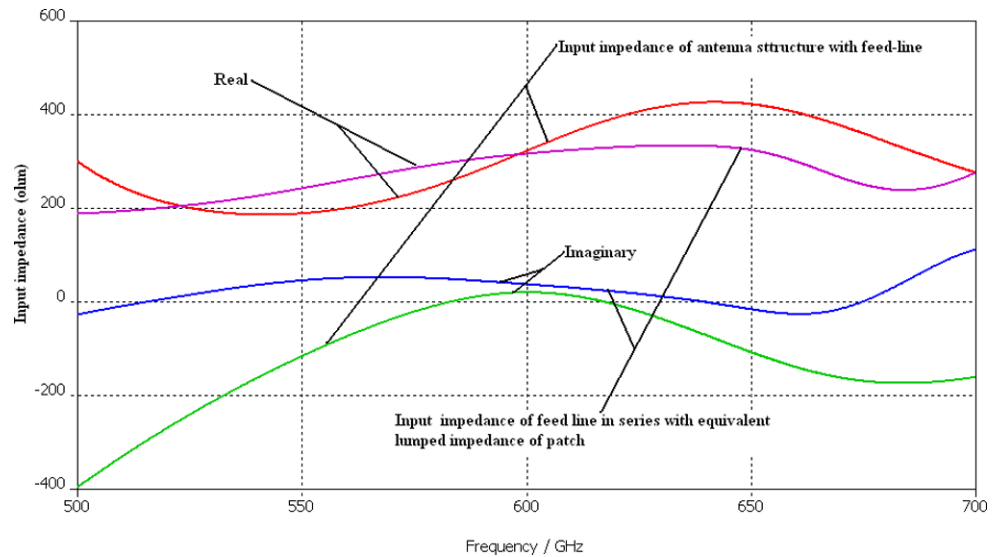
due to the capacitive nature of the patch. We have extracted the equivalent capacitive reactance of the patch by using (10) and (11) and have found it equal to 21.76Ω , which is again in the close agreement to the value shown in Fig. 3.

$$C = \frac{L_1}{Z_0 v_p} \quad (10)$$

$$Z = \frac{1}{j\omega C} \quad (11)$$

On this way, an equivalent circuit model of the radiating patch, which consists of resistance in series with capacitance, may be drawn. Next to this, the microstrip feed-line is modeled as a combination of inductance in series with resistance circuit. In a narrow microstrip transmission line, the accuracy of the impedance is inconsistent and tends to be high which cannot be determined by using the design formulas. To determine the impedance of the microstrip feed-line, we placed the equivalent lumped impedance of the radiating patch in series with the transmission line and obtained the input impedance of this combination at the port. Further, it is compared with the input impedance seen by the port when whole structure is simulated which is depicted in Fig. 4. From Fig. 4, it is seen that two impedances are close to each other at 600 GHz. By inspecting this figure, it is concluded that the behavior of the microstrip feed-line is inductive and its effective impedance is extracted by subtracting the patch impedance as shown in Fig. 3 from the impedance of the whole structure. The calculated value of the impedance of the microstrip feed-line is equal to $85 + j59.8$ and $91 + j42.53 \Omega$ in these two cases, respectively. These results are also in the close agreement at this high frequency. Further, it is believed that the antenna with feed-line can be modeled as series *RLC* network. From this analysis, it is also concluded that the antenna would resonate near 600 GHz where, the reactive component is close to zero. The exact analysis of the return loss of antenna is difficult due to variation in the characteristic impedance of the port. In

Fig. 4 The input impedance of the antenna at 600 GHz by using lumped element approach



general, the microstrip transmission-line formulas are extracted in the closed form. However, to investigate the radiation characteristics of antenna, it is necessary to operate the antenna in an open environment by adding open space above the radiating patch. The added space above the radiator influences the effective permittivity and the characteristic impedance of the antenna. The variation in effective permittivity is evident from Fig. 2 and when the wave port is used to excite the device in the CST Microwave Studio, it is considered that the port is matched to the device seen by the port at every frequency point. On this way, it is concluded that the line impedance seen by the port is nothing but the characteristic impedance of the port itself. To analyze the return loss, we have obtained the characteristic impedance of the port by selecting full deembedding radio button in the transient solver of the CST Microwave Studio and have extracted the return loss by using following formula.

$$RL = -20 \log |\Gamma| dB \quad \text{where } \Gamma = \frac{Z_{in} - Z_0}{Z_{in} + Z_0} \quad (12)$$

where, RL , Γ , Z_{in} and Z_0 are return loss, reflection coefficient, input impedance seen by the port and characteristic impedance of the port, respectively. In the above analysis, we have considered the impedance of the feed line in series with equivalent lumped impedance of the patch shown in Fig. 4 as Z_{in} . The analysis shows variation in the S_{11} parameter which is mainly due to the variation in the impedance of the patch in the analysis and simulation. However, both the results show a wide-band impedance bandwidth and minimum return loss near 600 GHz. To support the simulation obtained by CST Microwave Studio, which is based on finite integral method, the structure was re-simulated in Ansoft HFSS a commercial simulator based on the finite element technique, which

is in agreement to the previous simulation. These three results are shown in Fig. 5. The result can be improved by considering the input impedance of the circuit as the impedance of the antenna structure with feed-line as shown in Fig. 4.

From this proposed analysis, we can also predict about the electrical behavior of the antenna under the investigation. In an inset-fed microstrip patch antenna, the radiation resistance is associated to the input resistance of the antenna by the following formula [35, 36].

$$R_{in} = R_r \cos^2(\pi x_f / L_1) \quad \text{for } R_r \geq R_{in} \quad (13)$$

$$G_r = 1/R_r \quad (14)$$

$$D = \frac{2}{15G_r} \left(\frac{w_1}{\lambda_0} \right) \quad (15)$$

In the above equations, R_r , x_f , G_r and D are radiation resistance, inset distance from the radiating edge, radiation conductance and directivity of the antenna, respectively. In the present design, we have approximated the value of directivity of the antenna by letting $x_f = 0$, as the antenna is fed at the edge of the radiating slot. Based on the previous analysis of the input impedance of the radiating patch, which is equal to $R_{in} = 282 \Omega$, the analytical value of the directivity of the antenna is equal to 8.762 dBi, which is validated by simulating the structure by CST Microwave Studio and simulated directivity is equal to 9.396 dBi. The far-field radiation pattern of the antenna is shown in Fig. 6. The radiation pattern indicates that the antenna is directive in the principle H-plane and maximum gain and radiation efficiency are 7.968 dBi and 71.98%, respectively. The -3 dB beamwidth of the mean beam in the principle H- and E-plane are 7.2° and 102.8° , respectively.

Fig. 5 Variation of the S_{11} parameter (dB) of the proposed antenna

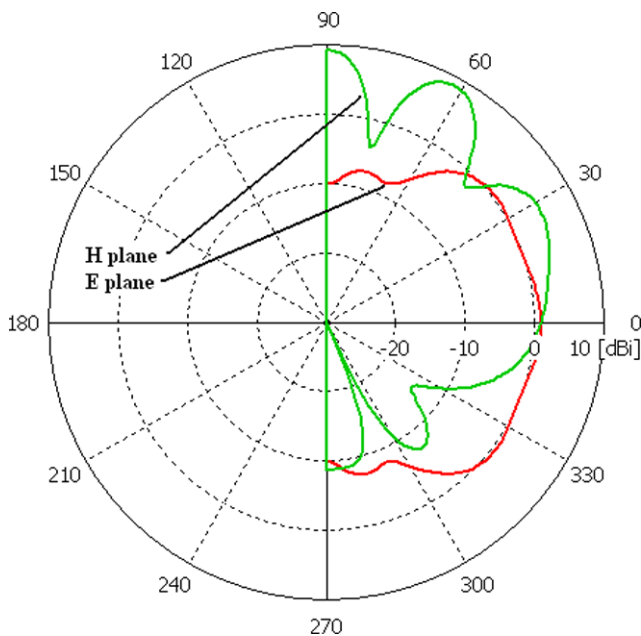
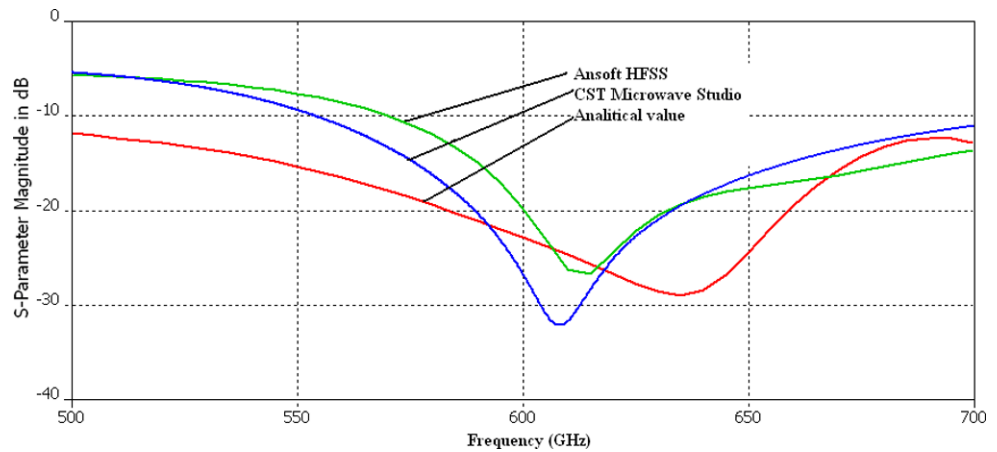


Fig. 6 Far-field radiation pattern of the proposed antenna at 600 GHz

4 Slow-wave antenna

From the series RLC model of the proposed antenna as discussed in the previous section, it is concluded that the resonance condition can be altered by simply adding a reactive component in the series. The addition of this reactive component would make the antenna suitable to operate in the wide range of the terahertz spectrum and addition of the inductive reactance would move the resonance condition to the higher frequency whereas addition of capacitive reactance would shift the frequency to lower side on the frequency axis in Fig. 5. However, the implementation of capacitive reactance is a better choice in comparison to the inductive impedance due to the constraint on the physical dimension. To analyze this effect, a series gap feeding technique is investigated in which the patch is fed by microstrip transmis-

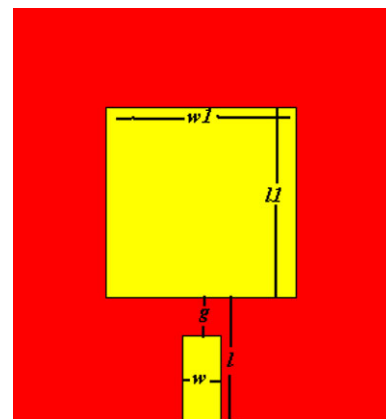


Fig. 7 Antenna structure with the gap-capacitance

sion line via a series gap of variable gap-length (g). The gap has been created by reducing the length of feed-line, which is shown in Fig. 7.

To investigate the effect of series capacitance loaded microstrip antenna, the gap distance is varied up to 10 μm in the 1 μm step size. This variation in the gap results the variation in the capacitance value. The net added capacitance in series is extracted by following approximate formulas [37].

$$C_g = 0.5C_o - 0.25C_e \tag{16}$$

$$\frac{C_o}{W} (\text{pF}/\text{m}) = \left(\frac{\epsilon_e(f)}{9.6}\right)^{0.8} \left(\frac{g}{W}\right)^{m_o} e^{k_o} \tag{17}$$

$$\frac{C_e}{W} (\text{pF}/\text{m}) = 12 \left(\frac{\epsilon_e(f)}{9.6}\right)^{0.9} \left(\frac{g}{W}\right)^{m_e} e^{k_e} \tag{18}$$

with

$$m_o = \frac{W}{h} [0.619 \log(W/h) - 0.3853] \tag{19}$$

$$k_o = 4.26 - 1.453 \log(W/h) \tag{20}$$

$$m_e = 0.8675 \tag{21}$$

Fig. 8 An extracted value of the gap-capacitance and impedance at 600 GHz

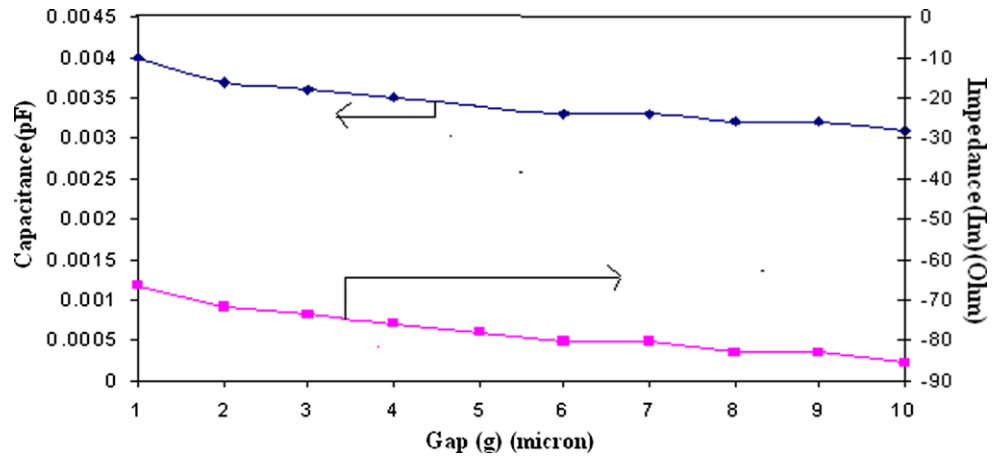


Fig. 9 Effect of gap distance between the feed-line and radiating patch on the S_{11} parameter

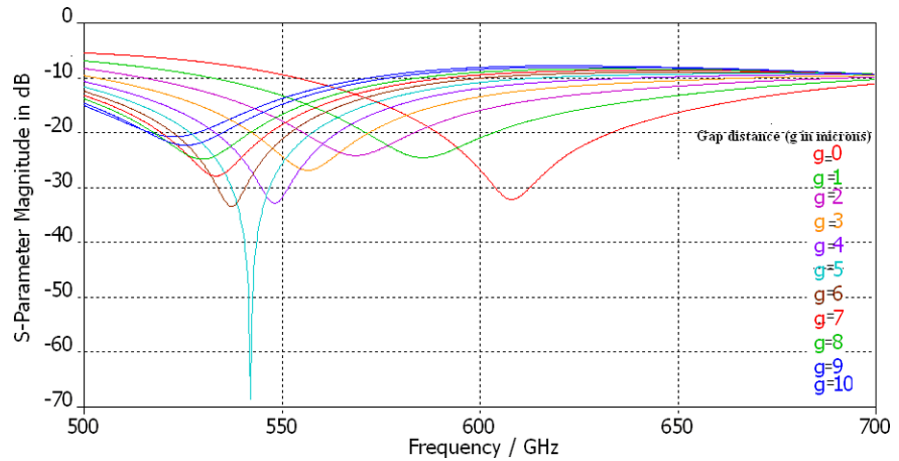
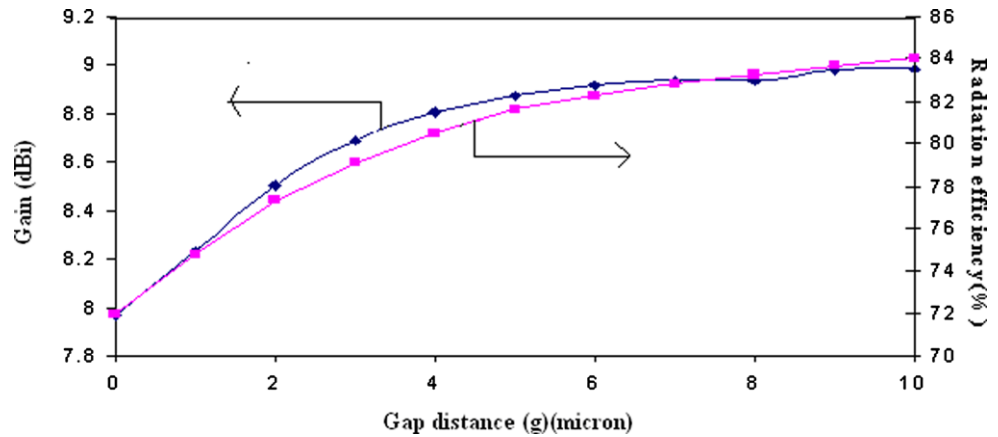


Fig. 10 An effect of the gap distance variation on the gain and radiation efficiency at 600 GHz



$$k_e = 2.043 \left(\frac{W}{h} \right)^{0.12} \quad (22)$$

In above equations, C_g , C_o and C_e are gap, odd-mode and even-mode capacitance of the gap, respectively. To extract the capacitance, radiating patch is considered as a transmission line whose width is equal to the width of the feed-

line. This assumption simplifies the analysis but a little error within reasonable limit may occur. The error would be insignificant due to the microscopic dimension of the antenna. In the above analysis, we have ignored the parallel parasitic capacitance between transmission-line and ground because of its insignificant value at terahertz frequency.

Figure 8 indicates that with increase in the gap distance, the series gap capacitance decreases and correspondingly reactive impedance (capacitive) increases at 600 GHz. Further, it reveals that the addition of negative impedance at this frequency causes the slope of reactive component of impedance as shown in Fig. 4 to change. On this way, cross-over point to zero reactive impedance shifts left (downshift). In other word, the resonance frequency is reduced below 600 GHz. It indicates that the behavior of the antenna can be changed to a slow-wave structure [38]. In a normal condition, to reduce the resonance frequency of the antenna, it is

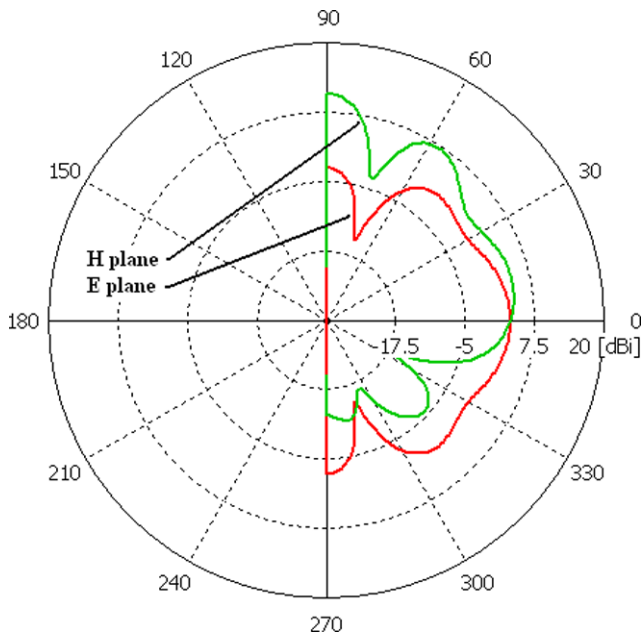


Fig. 11 Directivity radiation pattern of the proposed antenna at 542 GHz

required to increase the dimension of the radiator, but in the present case without altering this dimension, the resonance frequency is shifted to the lower frequency. The immediate advantage of this configuration is the compactness of the microstrip antenna. The effect of variation in the gap distance on the return loss parameter is shown in Fig. 9.

Apart from the variation in S -parameter, the gain/directivity and radiation efficiency increases monotonously which is shown in Fig. 10. In addition to shift in resonance condition, the return loss at 600 GHz increases towards -10 dB and this limits its application beyond certain value of the gap distance. From Fig. 9, it is concluded that the maximum resonance is obtained for the gap distance of $5 \mu\text{m}$ and structure optimally matched at 542 GHz. The radiation pattern at this frequency is shown in Fig. 11. The -3 dB mean beamwidth in this case in the principle H- and E-planes are 8.7° and 50.6° , respectively. The gain is increased mainly due to reduction in angular beam-width in E-plane.

From Fig. 11, it is clear that the antenna is directive in principle H-plane in comparison to principle E-plane. The directivity is maximum at $\phi = \theta = 90^\circ$. This result shows that the directivity of the antenna is equal to 10.94 dBi and other electrical parameters such as the gain and radiation efficiency are equal to 9.585 dBi and 73.12%, respectively. In this case, the directivity of the antenna is increased by 1.571 dB with respect to the directivity of the antenna at 600 GHz. In addition to this, the radiation efficiency is also increased up to 1.14%. The polarization effect of this antenna is shown in Fig. 12. From Fig. 12, it is seen that the cross-polarization is significantly less which is equal to about -315 dB in the whole range of elevation angle (θ) in the yz plane and also significantly less around $\theta = 0^\circ$ in

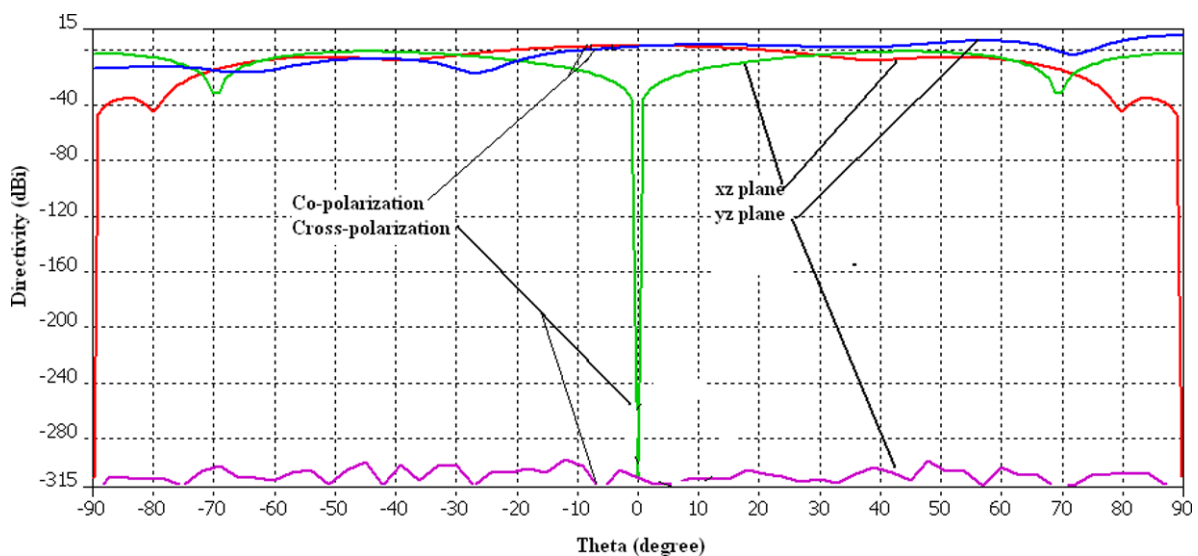


Fig. 12 Co- and cross-polarization of the antenna at 542 GHz

the xz plane. It indicates that the field would be the linearly polarized.

5 Conclusion

In this paper, an expression to calculate the effective dielectric permittivity of the two-layered substrate material at the terahertz frequency has been analyzed. Maximum deviation of analytical result with respect to frequency domain solver, full-wave calculator, eigenmode solver and transient solver is 0.427%, 1.41%, 1.14% and 2.09%, respectively. The deviation in result with respect to transient solver is attributed to the integration technique and simplification in capacitive model with addition to the open space above the patch. The maximum deviation in result of microstrip line and antenna (whole structure) when simulated using transient solver is equal to 1.29% which indicates that analysis of an effective dielectric permittivity performed on a simple microstrip line can be extended to the antenna structure with minimum error. Based on the above calculation, a rectangular microstrip antenna has been analyzed and simulated at 600 GHz. The slow-wave effect has been investigated on this proposed antenna, which is useful in designing a compact antenna. By using the slow-wave concept, another antenna has been analyzed and simulated at 542 GHz, which shows the potential improvement of the electrical performance. The methodology can also be extended to other topology in the terahertz spectrum.

Acknowledgements Authors are sincerely thankful to the potential reviewers for their critical comments and suggestions to improve the quality of the manuscript.

References

1. Siegel, P.H.: Terahertz technology. *IEEE Trans. Microw. Theory Tech.* **50**(3), 910–928 (2002)
2. Zhong, H., Redo-Sanchez, A., Zhang, S.-C.: Identification and classification of chemicals using terahertz reflective spectroscopic focal plane imaging system. *Opt. Express* **14**, 9130–9141 (2006)
3. Choi, M.K., Bettermann, A.D., van der Weide, D.W.: Potential for detection of explosive and biological hazards with electronic terahertz systems. *Philos. Trans. R. Soc. Lond. A* **362**, 337–349 (2004)
4. Galoda, S., Singh, G.: Fighting terrorism with terahertz. *IEEE Potential Mag.* **26**(6), 24–29 (2007)
5. Choi, M.K., Taylor, K., Bettermann, A., van der Weide, D.W.: Broadband 10–300 GHz stimulus response sensing for chemical and biological entities. *Phys. Med. Biol.* **47**, 3777–3787 (2002)
6. Woolard, D.L., Brown, R., Pepper, M., Kemp, M.: Terahertz frequency sensing and imaging: a time of reckoning future applications? *Proc. IEEE* **93**(10), 1722–1743 (2005)
7. Fitzgerald, J., Berry, E., Zinovev, N.N., Walker, G.C., Smith, M.A., Chamberlain, J.M.: An introduction to medical imaging with coherent terahertz frequency radiation. *Phys. Med. Biol.* **47**, R67–R84 (2002)
8. Ozbay, E., Temelkuran, B., Bayindir, M.: Microwave applications of photonic crystals. *Prog. Electromagn. Res.* **41**, 185–209 (2003)
9. Gonzalo, R., Martinez, B.: The effect of dielectric permittivity on the properties of photonic band gap devices. *Microw. Opt. Technol. Lett.* **23**(2), 92–95 (1999)
10. Gonzalo, R.: Enhanced patch-antenna performance by suppressing surface waves using photonic-band gap substrates. *IEEE Trans. Microw. Theory Tech.* **47**(11), 2131–2138 (1999)
11. Yang, H.Y.D., Alexopoulos, N.G., Yablonovitch, E.: Photonic band gap materials for high gain printed circuit antennas. *IEEE Trans. Antennas Propag.* **45**(1), 185–187 (1997)
12. Fernandes, H.C.C., da Rocha, A.R.B.: Analysis of antennas with PBG substrate. *Int. J. Infrared Millim. Waves* **24**(7), 1171–1176 (2003)
13. Brown, E.R., Parker, C.D.: Radiation properties of a planar antenna on a photonic-crystal substrate. *J. Opt. Soc. Am. B* **10**(2), 404–407 (1993)
14. Dahele, J.S., Lee, K.F., Wong, D.P.: Dual-frequency stacked annular-ring microstrip antenna. *IEEE Trans. Antennas Propag.* **35**(11), 1281–1285 (1987)
15. Halim, B., Denidni, T.A.: Gain enhancement of microstrip patch antenna using a cylindrical electromagnetic crystal substrate. *IEEE Trans. Antennas Propag.* **55**(11), 3140–3145 (2007)
16. Noghianian, S., Shafai, L.: Gain enhancement of annular slot antennas. *IEE Proc. Microw. Antennas Propag.* **148**(2), 109–114 (2001)
17. Nishiyama, E., Aikawa, M., Egashira, S.: Stacked microstrip antenna for wideband and high gain. *IEE Proc. Microw. Antennas Propag.* **151**(2), 143–148 (2004)
18. Kumar, P., Singh, G.: Theoretical investigation of the input impedance of gap-coupled circular microstrip patch antennas. *J. Infrared Millim. Terahertz* **30**(11), 1148–1160 (2009)
19. Croq, F., Pozar, D.M.: Multi-frequency operation of microstrip antennas using aperture coupled parallel resonators. *IEEE Trans. Antennas Propag.* **40**(11), 1367–1374 (1992)
20. Richards, W.F., Davidson, S.E., Long, S.A.: Dual-band reactively loaded microstrip antenna. *IEEE Trans. Antennas Propag.* **33**(5), 556–560 (1985)
21. Davidson, S.E., Long, S.A., Richards, W.F.: Dual-band microstrip antenna with monolithic reactive loading. *Electron. Lett.* **21**(21), 936–937 (1985)
22. Lee, R.Q., Lee, K.F.: Gain enhancement of microstrip antennas with overlying parasitic directors. *Electron. Lett.* **24**(11), 656–658 (1998)
23. Sharma, A., Singh, G.: Design of single pin shorted three dielectric-layered substrates rectangular patch microstrip antenna for communication systems. *Prog. Electromagn. Res. Lett.* **2**, 157–165 (2008)
24. Sharma, A., Singh, G., Chauhan, D.S.: Design considerations to improve the performance of a rectangular microstrip patch antenna at THz frequency. In: *Proc. 33rd International Conference on Infrared, Millimeter, and Terahertz Waves, USA*, pp. 1–2, 15–19th Sept. 2008
25. Singh, G.: Design consideration for rectangular microstrip patch antenna on electromagnetic crystal substrate at terahertz frequency. *Infrared Phys. Technol.* **53**(1), 17–22 (2010)
26. Jha, K.R., Singh, G.: Dual-band rectangular microstrip patch antenna at terahertz frequency for surveillance system. *J. Comput. Electron.* **9**(1), 31–41 (2010)
27. Svacina, J.: Analysis of multilayer microstrip lines by a conformal mapping method. *IEEE Trans. Microw. Theory Tech.* **40**(4), 769–772 (1992)
28. Verma, A.K., Sadr, G.H.: Unified dispersion model for multilayer microstrip line. *IEEE Trans. Microw. Theory Tech.* **40**(7), 1587–1591 (1992)

29. Jansen, R.H.: A novel CAD tool ad concept compatible with the requirements of multilayer GaAs MMIC technology. In: Proc. IEEE MTT-S Microw. Symp. Dig., pp. 711–714 (1980)
30. Hilberg, W.: From approximation to exact relations for characteristic impedances. IEEE Trans. Microw. Theory Tech. **17**(5), 259–265 (1969)
31. Kirschning, M., Jansen, R.H.: Accurate model for effective dielectric constant of microstrip with validity up to millimeter-wave frequencies. Electron. Lett. **18**(6), 272–273 (1982)
32. Hammerstad, E., Jensen, O.: Accurate models for microstrip computer aided design. In: 1980 IEEE MTT-S Int. Microw. Symp. Dig., USA, pp. 407–409 (1980)
33. Kobayshi, M.: A dispersive formula satisfying recent requirements in microstrip CAD. IEEE Trans. Microw. Theory Tech. **36**(8), 1246–1250 (1988)
34. Iskander, M.F.: Electromagnetic Fields and Waves. Prentice-Hall, New York (1992)
35. Balanis, C.A.: Antenna Theory Analysis and Design. Wiley, New York (2001)
36. Garg, R., Bhartia, P., Bahl, I., Ittipiboon, A.: Microstrip Antenna Design Handbook. Artech House, Norwood (2001)
37. Gupta, K.C., Garg, R., Bahl, I., Bhartis, P.: Microstrip Lines and Slot-Lines, 2nd edn. Artech House, Norwood (1996)
38. Jha, K.R., Rai, M.: A slow wave structure and its application in band pass filter design. AEU Int. J. Electron. Commun. **64**(2), 177–185 (2010)